TWO-PHASE LIQUID–LIQUID ANNULAR FLOW

N. Brauner

Department of Fluid Mechanics and Heat Transfer, School of Engineering, Tel-Aviv University,
Ramat Aviv, Tel-Aviv 69978, Israel

Abstract—A simple predictive tool for analyzing the annular-core flow of two immiscible liquids is presented. The model puts under a common framework all possible flow situations of laminar–laminar, turbulent–turbulent or mixed flow regimes in the two phases involved for wide ranges of viscosity and density ratios. Comparison with available experimental data of pressure drop and *in situ* hold-up shows a satisfactory agreement.

The potential of the core flow configuration for achieving pressure loss reduction and power saving in the transportation of very viscous oils is evaluated, addressing the problem of tube size scale-up.

Key Words: annular flow, core flow, liquid–liquid, oil–water, two-phase

1. INTRODUCTION

The contact of two immiscible liquids is encountered widely in the chemical and petroleum industries. Although there is a considerable amount of published information on the flow of liquid–gas and liquid–solid mixtures, there is relatively very little on the flow of liquid–liquid mixtures.

In liquid–liquid flows, as in gas–liquid systems, the two phases can be distributed in the conduit in many configurations called flow patterns, differing from each other in the spatial distribution of the interface. The flow pattern depends on the operational variables, physical properties of the fluids and geometrical variables of the system.

One of the flow patterns, which appears most attractive from the viewpoint of pressure loss reduction in liquid transportation lines, is that of the central core flow of highly viscous fluid, while the less viscous liquid (water) forms a uniform annulus in the region of high shear rate next to the pipe wall.

The annular (water and oil) core pattern, or simply core flow, being the one of most interest in technological processes, has drawn attention during the last two decades. The theoretical studies of core flow can be divided into two main groups: the first includes studies which utilize the general concept of encapsulation of solids or highly viscous liquids in a stream of less viscous fluid; in the second group, direct solutions of the two fluids hydrodynamic or instability equations are most common.

Charles (1963) presented a theoretical analysis of concentric flow of cylindrical capsules in laminar or turbulent annuli. This study was followed by several experimental studies (Ellis 1964a,b; Ellis & Bolt 1964; Round & Bolt 1965) on the transport of single cylindrical or spherical capsules in a stream of water. In parallel, numerical analyses for laminar flow around free cylindrical capsules (Newton *et al.* 1964; Kruyer *et al.* 1967) or fixed eccentric cores (Redberger & Charles 1962), have also been reported. These studies are relevant to liquid–liquid annular flow when the core viscosity goes to infinity.

Attempts to diverge from the capsule model and solve for the flow fields in both the core and the annular gap have been presented by Russell & Charles (1959), Bentwich (1964) and Bentwich *et al.* (1970). The analyses refer to the velocity fields for fully developed laminar motion in *smooth* annular concentric or eccentric flows.

A rather different direction is represented by a series of theoretical studies by Ooms & Beckers (1972), and later on by Ooms *et al.* (1984, 1985) and Oliemans (1986). Ooms (1972) considered the hydrodynamic stability of core–annular flow of two ideal liquids with a smooth interface in

horizontal pipes. It was concluded that the core–annular flow of two ideal liquids is hydrodynamically unstable, whereby the interface becomes rippled. In parallel, Ooms & Beckers (1972), and later Ooms *et al.* (1984, 1985), consider the annular flow surrounding a rigid core by resorting to laminar hydrodynamic lubrication theory, and assuming the existence of highly nonsymmetric waves on the core surface. This approach was recently extended by Oliemans (1986) to a turbulent lubrication model. These models are numerically complicated and also require as input the annular layer thickness and the interfacial waviness characteristics (which are to be modeled or measured at the flow conditions under consideration).

The role of the interfacial waviness in counterbalancing the buoyancy of an oil core flowing in a water annulus is widely dealt with in a subsequent paper (Moalem Maron *et al.* 1990), where the stabilizing mechanisms of core flow are explored. The transitions to other liquid–liquid flow patterns are the concern of separate studies (Brauner & Moalem Maron 1990, 1991a–c). Here, however, the main objective is to present a simple practical prediction tool for general annular liquid–liquid flow. As distinct from previous related studies, which are concerned with either solid capsule flow (Charles 1963; Oliemans 1986) or are restricted to laminar–laminar flow regimes, the approach proposed herein represents an attempt to put under a common frame all possible flow regime combinations in the annular and core phases. As is shown, the approach, though based on the average two fluid quantities, still points out all the main features of the annular liquid–liquid flow pattern for a wide range of liquid–liquid systems.

2. PHYSICAL MODEL AND GOVERNING EQUATIONS

Consider an annular flow configuration of two immiscible fluids, a and b, in a horizontal or slightly inclined conduit, as illustrated in figure 1. Assuming fully developed flow, the integral forms of the momentum equations for the core (c) and annular (w) regions are:

$$-A_c\left(\frac{dP}{dx}\right) \mp \tau_i S_i + \rho_c A_c g \sin \beta = 0; \qquad \text{core region;} \qquad [1]$$

and

$$-A_w\left(\frac{dP}{dx}\right) - \tau_w S_w \pm \tau_i S_i + \rho_w A_w g \sin \beta = 0; \qquad \text{wall region;} \qquad [2]$$

with

$$\rho_c = \rho_a \alpha_c + \rho_b(1 - \alpha_c); \qquad \alpha_c = \frac{A_{ac}}{A_c}; \qquad [3]$$

and

$$\rho_w = \rho_b \alpha_w + \rho_a(1 - \alpha_w); \qquad \alpha_w = \frac{A_{bw}}{A_w}; \qquad [4]$$
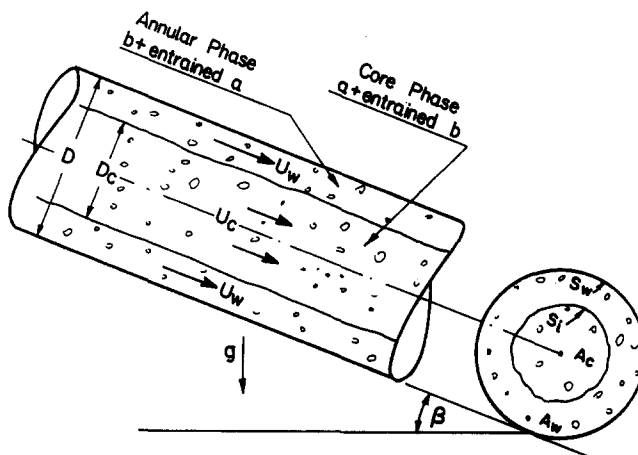
Figure 1. Schematic description of two-phase annular flow.

where the upper signs in [1] and [2] correspond to a faster flowing core region and A_c, A_w, ρ_c and ρ_w are the flow areas and equivalent densities of the core and annular (wall) regions due to entrainment of $(1 - \alpha_c)$ of phase b into a and $(1 - \alpha_w)$ of phase a into phase b. Thus, for a pure core phase a and a pure annular phase b, $\alpha_c = \alpha_w = 1$. Eliminating the pressure gradient, dP/dx, yields:

$$-\tau_w \frac{S_w}{A_w} \pm \tau_i S_i \left(\frac{1}{A_c} + \frac{1}{A_w}\right) + (\rho_w - \rho_c)g \sin \beta = 0. \qquad [5]$$

As conventionally used in two-fluid models, the wall shear stress τ_w is expressed in terms of the corresponding friction factors f_w based on the annulus hydraulic diameter D_w and the corresponding Reynolds numbers:

$$\tau_w = f_w \frac{\rho_w U_w^2}{2}; \quad f_w = C_w \left(\frac{D_w U_w}{\nu_w}\right)^{-n_w}; \quad D_w = \frac{4A_w}{S_w}; \qquad [6]$$

where S_w is the perimeter of the wall. Note that, in view of [6], the wall friction factor, f_w, is determined by the *a priori* unknown actual annular thickness and velocity, U_w. These, in turn, are evaluated (among other flow variables) taking into account the mutual interaction between the two phases, e.g. the interfacial shear and the relative velocities.

As distinct from stratified flow, where the velocity of one phase may alternatively exceed the other (Brauner & Moalem Maron 1989), in a horizontal (or slightly downward inclined) annular flow, the core velocity ought to be higher than the annular phase velocity in order to satisfy [1]. Consequently, the hydraulic diameter for the annular phase, D_w, is defined in [6] as for a free interface, and only the upper signs in [1] and [2] are relevant. The interfacial shear stress between the two phases, τ_i, is evaluated by

$$\tau_i = f_i \frac{\rho_c (U_c - U_w)^2}{2}; \quad f_i = BC_c \left(\frac{D_c U_c}{\nu_c}\right)^{-n_c}. \qquad [7]$$

In [6] and [7] the constants C_c, C_w, n_w and n_c are chosen according to the flow regime in each phase. Clearly, the two phases in annular flow may be in laminar–laminar (L–L), laminar–turbulent (L–T), turbulent–laminar (T–L) or turbulent–turbulent (T–T) regimes. These constants are given the following values: $C = 16$ and $n = 1$ for laminar flow; and $C = 0.046$ and $n = 0.2$ for turbulent flow conditions. B denotes the augmentation of the interfacial shear due to interfacial waviness.

In the modeling of gas–liquid flows where $U_c \equiv U_G \gg U_w$, the slower velocity U_w in [7] is sometimes replaced by the interfacial velocity. Here, however, consistent with the two-fluid model used, where the velocity profiles are unresolved, average velocities are used. Also, in liquid–liquid systems the interface appears less roughened and is characterized by long smooth waves, and thus the augmentation of the interfacial shear factor due to waviness is ignored ($B = 1$). Moreover, as the velocities of the two phases in liquid–liquid systems are comparable, the modeling becomes even less sensitive to the estimation of the interfacial friction factor.

In order to express the actual region velocities, U_w and U_c, in terms of input flow rates and *in situ* hold-up, overall mass balances on the two fluids a and b are formulated (assuming no slip between the phases in each region):

$$A U_{as} = U_w A_w (1 - \alpha_w) + U_c A_c \alpha_c; \quad U_{as} = \frac{Q_a}{A}; \qquad [8a]$$

and

$$A U_{bs} = U_w A_w \alpha_w + U_c A_c (1 - \alpha_c); \quad U_{bs} = \frac{Q_b}{A}; \qquad [8b]$$

which yield

$$\tilde{U}_c = \frac{U_c}{U_{as}} = \frac{\tilde{A}}{\tilde{A}_c} \frac{(1 - \alpha_w) - \phi \alpha_w}{\phi [1 - (\alpha_c + \alpha_w)]} \qquad [9a]$$

and

$$\tilde{U}_{\mathrm{w}} = \frac{U_{\mathrm{w}}}{U_{bs}} = \frac{\tilde{A}}{\tilde{A}_{\mathrm{w}}} \frac{\alpha_c - (1 - \alpha_c)\phi}{\alpha_c + \alpha_{\mathrm{w}} - 1},$$ [9b]

where

$$\phi = \frac{U_{as}}{U_{bs}};$$ [9c]

with U_{as} and U_{bs} being the superficial velocities of the fluids involved. The geometric non-dimensional variables are defined by

$$\tilde{D}_{\mathrm{c}} = \frac{D_{\mathrm{c}}}{D}; \quad \tilde{S}_{\mathrm{i}} = \frac{S_{\mathrm{i}}}{D} = \pi\tilde{D}_{\mathrm{c}}; \quad \tilde{S}_{\mathrm{w}} = \frac{S_{\mathrm{w}}}{D} = \pi;$$

$$\tilde{A} = \frac{A}{D^2} = \frac{\pi}{4}; \quad \tilde{A}_{\mathrm{c}} = \frac{A_{\mathrm{c}}}{D^2} = \frac{\pi}{4}\tilde{D}_{\mathrm{c}}^2; \quad \tilde{A}_{\mathrm{w}} = \frac{A_{\mathrm{w}}}{D^2} = \frac{\pi}{4}(1 - \tilde{D}_{\mathrm{c}}^2);$$ [10]

$$\tilde{D}_{\mathrm{w}} = \frac{4\tilde{A}_{\mathrm{w}}}{\tilde{S}_{\mathrm{w}}} = 1 - \tilde{D}_{\mathrm{c}}^2.$$

Introducing nondimensional variables and substituting [6] and [7] into [5], the normalized form of the latter reads:

$$\frac{\rho_c}{\rho_a}\left(\frac{v_a}{v_c}\tilde{D}_{\mathrm{c}}\tilde{U}_{\mathrm{c}}\right)^{-n_c}\left(1 - \frac{1}{\phi}\frac{\tilde{U}_{\mathrm{w}}}{\tilde{U}_{\mathrm{c}}}\right)^2\left(\frac{1}{\tilde{A}_{\mathrm{w}}} + \frac{1}{\tilde{A}_{\mathrm{c}}}\right)\tilde{S}_{\mathrm{i}}\tilde{U}_{\mathrm{c}}^2 - \frac{\rho_w}{\rho_b}\chi^2\left(\frac{v_b}{v_w}\tilde{D}_{\mathrm{w}}\tilde{U}_{\mathrm{w}}\right)^{-n_w}\frac{\tilde{S}_{\mathrm{w}}}{\tilde{A}_{\mathrm{w}}}\tilde{U}_{\mathrm{w}}^2 + 4Y = 0.$$ [11]

The two-phase flow parameters χ^2 and Y evolve through the normalization of [5] and are given by

$$\chi^2 = \frac{\left(\dfrac{4C_{\mathrm{w}}}{D}\right)\left(\dfrac{U_{bs}D}{v_b}\right)^{n_w}\dfrac{\rho_b U_{bs}^2}{2}}{\left(\dfrac{4C_{\mathrm{c}}}{D}\right)\left(\dfrac{U_{as}D}{v_a}\right)^{n_c}\dfrac{\rho_a U_{as}^2}{2}}$$ [12a]

and

$$Y = \frac{(\rho_w - \rho_c)g\sin\beta}{\left(\dfrac{4C_{\mathrm{c}}}{D}\right)\left(\dfrac{U_{as}D}{v_a}\right)^{n_c}\dfrac{\rho_a U_{as}^2}{2}}.$$ [12b]

Since the various geometric parameters and the nondimensional velocities, $\tilde{U}_{\mathrm{c}}$ and $\tilde{U}_{\mathrm{w}}$, are all functions of the core diameter, $\tilde{D}_{\mathrm{c}}$, [11] states, in general that

$$\tilde{D}_{\mathrm{c}} = f(\chi^2, Y, \phi, n_{\mathrm{c}}, n_{\mathrm{w}}, \alpha_{\mathrm{c}}, \alpha_{\mathrm{w}}),$$ [13]

where n_{c} and n_{w} stand for the actual flow regime parameters of the two phases and are determined through the solution.

The two-phase pressure gradient is obtained, as usual, by eliminating τ_{i} from [1] and [2], whereby, in dimensionless form, it is given by

$$\Phi_a = \frac{-\left(\dfrac{\mathrm{d}P}{\mathrm{d}x}\right)}{\left(\dfrac{4C_{\mathrm{c}}}{D}\right)\left(\dfrac{U_{as}D}{v_a}\right)^{n_c}\dfrac{\rho_a U_{as}^2}{2}} = \frac{1}{4}\chi^2\frac{\rho_w}{\rho_b}\frac{\tilde{S}_{\mathrm{w}}\tilde{U}_{\mathrm{w}}^2}{\tilde{A}}\left(\frac{v_b}{v_w}\tilde{D}_{\mathrm{w}}\tilde{U}_{\mathrm{w}}\right)^{-n_w} - \tilde{\rho}Y$$ [14a]

and

$$\Phi_b = \frac{-\left(\dfrac{\mathrm{d}P}{\mathrm{d}x}\right)}{\left(\dfrac{4C_{\mathrm{w}}}{D}\right)\left(\dfrac{U_{bs}D}{v_b}\right)^{n_w}\dfrac{\rho_b U_{bs}^2}{2}} = \frac{\Phi_a}{\chi^2},$$ [14b]

with

$$\tilde{\rho} = \frac{\rho_c \tilde{A}_c + \rho_w \tilde{A}_w}{(\tilde{A}_c + \tilde{A}_w)(\rho_w - \rho_c)}.$$ [15]

In [14a,b], Φ_a and Φ_b represent the references of the two-phase pressure gradient to either of the two fluids. From the application point of view, it is very common to refer the two-phase pressure drop to that which would have been obtained with the less viscous fluid (b) flowing alone at the two-phase mixture velocity, whereby

$$\Pi = \frac{\left(\dfrac{dP}{dx}\right)_{TP}}{\left(\dfrac{dP}{dx}\right)_s}; \qquad \left(\frac{dP}{dx}\right)_s = \frac{4}{D}\frac{f_s \rho_b (U_{as} + U_{bs})^2}{2}$$

$$f_s = C_s \left[\frac{D(U_{as} + U_{bs})}{v_b}\right]^{-n_s}.$$ [16]

Since this reference (superficial) flow is practically always in the turbulent regime (with $C_s = 0.046$ and $n_s = 0.2$), Π may be simply related to Φ_b (or to Φ_a, see [14b]):

$$\Pi = \frac{16}{0.046}\Phi_b \, \mathrm{Re}_{bs}^{-0.8}(1 + \phi)^{-1.8}; \qquad \text{laminar } b;$$ [17a]

$$\Pi = \Phi_b (1 + \phi)^{-1.8}; \qquad \text{turbulent } b.$$ [17b]

Whereas Φ_a expresses the pressure reduction associated with the transportation of viscous fluids in a core flow configuration, the Π factor points out the extent of increase expected in the two-phase pressure drop in relation to the value based on a single-phase flow of the less viscous fluid at the total (two-phase) flow rate.

It is to be emphasized that the denominators in [14a,b], although including superficial Reynolds numbers, do not always represent the "superficial" pressure drops of the phase involved (as usually stated in the literature), since the constants C_c and n_c or C_w and n_w are determined according to the *actual* flow regimes when the two (annular and core) phases coexist. Similarly, the definitions of χ^2 and Y in [12a,b], as they have evolved from the normalization procedure, include again superficial Reynolds numbers, but also initially-unknown actual two-phase parameters. Thus, Φ_a, Φ_b, χ^2 and Y include mixed superficial and actual parameters. For convenience of applicability it is therefore suggested here to present the results below in terms of χ_s^2, the Lockhart–Martinelli parameter, which is fully based on superficial variables:

$$\chi_s^2 = \frac{\left(\dfrac{dP}{dx}\right)_{bs}}{\left(\dfrac{dP}{dx}\right)_{as}} = \chi^2 \frac{\dfrac{C_{bs}}{C_w}\mathrm{Re}_{as}^{-(n_{bs} - n_w)}}{\dfrac{C_{as}}{C_c}\mathrm{Re}_{bs}^{-(n_{as} - n_c)}}.$$ [18]

Here n_{as}, n_{bs}, C_{as} and C_{bs} are determined based on the superficial Reynolds numbers, Re_{as} and Re_{bs}, of each fluid and, in principle, may be different from the corresponding actual values. The flow regime may be laminar in one phase, while turbulent in the other. However, in the range of sufficiently low flow rates, where the two phases are laminar based on both the actual and superficial Reynolds numbers, [18] yields $\chi_s^2 \equiv \chi^2$. Similarly, for sufficiently high flow rates, where turbulent regimes prevail in both phases, actual χ^2 and superficial χ_s^2 are identical. In between these two extremes there exist flow rate ranges for the two phases where χ^2 may be different from χ_s^2.

As indicated by [11] and [14a,b], or simply by [13], the solution is obtained in terms of χ_s^2, Y and ϕ. For horizontal flow, only χ_s^2 and ϕ remain (assuming α_c and α_w to be known). Consistent with the above, in the L–L and T–T extremes, [12a] and [18] reduce to:

$$\chi_s^2 = \frac{\mu_b}{\mu_a}\frac{1}{\phi}; \qquad \qquad \mathrm{L}(a)\text{–}\mathrm{L}(b);$$ [19]

and

$$\chi_s^2 = \left(\frac{\mu_b}{\mu_a}\right)^{0.2}\left(\frac{\rho_b}{\rho_a}\right)^{0.8}\frac{1}{\phi^{1.8}} = \left(\frac{\mu_b}{\mu_a}\right)\left(\frac{v_a}{v_b}\right)^{0.8}\frac{1}{\phi^{1.8}}; \qquad \mathrm{T}(a)\text{–}\mathrm{T}(b);$$ [20]

while for mixed flow regimes:

$$\chi_s^2 = \frac{16}{0.046} \frac{\mu_b}{\mu_a} \frac{1}{\phi} \, \mathrm{Re}_{as}^{-0.8} = \frac{16}{0.046} \left(\frac{\mu_b}{\mu_a}\right)^{0.2} \left(\frac{\rho_b}{\rho_a}\right)^{0.8} \frac{1}{\phi^{1.8}} \, \mathrm{Re}_{bs}^{-0.8}; \quad L(b)\text{-}T(a);$$ [21]

and

$$\chi_s^2 = \frac{0.046}{16} \frac{\mu_b}{\mu_a} \frac{1}{\phi} \, \mathrm{Re}_{bs}^{0.8} = \frac{0.046}{16} \left(\frac{\mu_b}{\mu_a}\right)^{0.2} \left(\frac{\rho_b}{\rho_a}\right)^{0.8} \frac{1}{\phi^{1.8}} \, \mathrm{Re}_{as}^{0.8}; \quad L(a)\text{-}T(b).$$ [22]

As noted above, whenever the superficial and actual flow regimes are identical, [19]–[22] are valid for χ^2 as well.

For a given L–L or T–T annular flow, the $\phi - \chi_s^2$ are not independent parameters and χ_s^2 is determined by ϕ (and vice versa) as indicated by [19] and [20]. However, in the case of mixed flow regimes, as in L–T or T–L, the relationships between ϕ and χ_s^2 include also the superficial Re number of the phases, and thus χ_s^2 and ϕ are two *independent* parameters of the given system. Also, for various two-fluid systems the relationships between χ_s^2 and ϕ quantitatively change according to the viscosity and density ratios of the fluid pair. For L–L conditions, the $\chi_s^2 - \phi$ dependence is not affected by the density ratio, and hence, still identical results for systems of different density ratios are expected. It is to be noted, however, when a gas–liquid system is considered, ϕ does not appear explicitly in [11] (or [13]) due to the $U_c \gg U_w$ assumption. Consequently, whereas gas–liquid nondimensional pressure drop and hold-up data in horizontal tubes are well-correlated by a single parameter, χ, liquid–liquid systems generally depend on both χ and ϕ.

3. CALCULATION PROCEDURE AND ANALYTICAL SOLUTIONS

Given an annular flow system (flow rates, physical properties, tube diameter), the variables in [11] can all be expressed in terms of $\tilde{D}_c$. As implied by [13], a solution for $\tilde{D}_c$ can be obtained provided α_c and α_w are prescribed from experimental observations or from separate modeling for the mutual extrainment between the phases. The solution procedure is in fact of an iterative nature, since the parameters n_c, n_w, C_c and C_w, which refer to the actual flow regimes, are determined through the iterative procedure.

Fortunately, for the case of a horizontal laminar core (with either a laminar or turbulent annular phase), simple explicit solutions for the *in situ* hold-up, $\tilde{D}_c$, and the resulting pressure drop are obtained. These are summarized in table 1.

Convergence to capsule flow models

For a very viscous oil core, where $\mu_b/\mu_a \to 0$, the solutions for $\tilde{D}_c$ and Φ_a for a laminar or turbulent annular layer (given in table 1) reduce to:

$$\tilde{D}_c = \left(\frac{\phi}{\phi + 1}\right)^{1/2}; \quad \frac{A_w}{A} = 1 - \tilde{D}_c^2 = \frac{1}{\phi + 1} = \frac{U_{bs}}{U_{as} + U_{bs}} = R;$$ [23]

$$\Phi_a = \frac{\mu_b}{\mu_a} \frac{(\phi + 1)^2}{\phi}; \quad \Phi_b = (\phi + 1)^2; \quad \Pi = \frac{16}{0.046} \, \mathrm{Re}_{bs}^{-0.8}(1 + \phi)^{0.2}; \quad \text{laminar } b;$$ [24a]

and

$$\Phi_a = \frac{0.046}{16} \frac{\mu_b}{\mu_a} \mathrm{Re}_{bs}^{0.8} \frac{(\phi + 1)^2}{\phi}; \quad \Phi_b = (\phi + 1)^2; \quad \Pi = (1 + \phi)^{0.2}; \quad \text{turbulent } b.$$ [24b]

Expressions [23] indicate that in the limit of a high viscous core, the *in situ* hold-up of the less viscous phase (usually water) approaches its input volumetric ratio, R, and the *in situ* velocities of both phases approach the mixture velocity. This bound is consistent with the experimental findings by Oliemans (1986). The two-phase pressure reduction factor (Φ_a^{-1} of [24a,b]) increases linearly with the two-phase viscosity ratio.

Optimal conditions

The conditions under which a maximum pressure reduction is achieved by the addition of the annular, less viscous, phase are obtained by exploring $\partial \Phi_a / \partial \phi = 0$. Simple analytic expressions for

Table 1. Core diameter and pressure drop for laminar core flow

	$\alpha_c, \alpha_w \neq 1$	$\alpha_c, \alpha_w = 1$
$L(c)$–$L(w)$	$\tilde{D}_c = \left\{ \dfrac{\phi}{\left[\dfrac{\mu_w}{\mu_c}\phi\dfrac{G(\phi)}{F(\phi)}\right]^{1/2} + \phi + \dfrac{G(\phi)}{F(\phi)}} \right\}^{1/2}$ $F(\phi) = \dfrac{\alpha_w \phi - (1-\alpha_w)}{\phi[\alpha_c + \alpha_w - 1]}; \quad G(\phi) = \dfrac{\alpha_c - (1-\alpha_c)\phi}{\alpha_c + \alpha_w - 1}$ $\Phi_a = \dfrac{\mu_w}{\mu_a}\dfrac{F^2(\phi)}{\phi G(\phi)} \left\{ \dfrac{\left[\dfrac{\mu_w}{\mu_c}\phi\dfrac{G(\phi)}{F(\phi)}\right]^{1/2} + \phi + \dfrac{G(\phi)}{F(\phi)}}{\left[\dfrac{\mu_w}{\mu_c}\phi\dfrac{F(\phi)}{G(\phi)}\right]^{1/2} + 1} \right\}^2$	$\tilde{D}_c = \left[\dfrac{\phi}{(\phi K_1)^{1/2} + \phi + 1} \right]^{1/2}$ $K_1 = \dfrac{\mu_b}{\mu_a}$ $\Phi_a = \dfrac{K_1}{\phi}\left[\dfrac{(K_1\phi)^{1/2} + \phi + 1}{(\phi K_1)^{1/2} + 1} \right]^2$
$L(c)$–$T(w)$	$\tilde{D}_c = \left\{ \dfrac{\phi}{\chi\phi\left[\dfrac{\mu_a}{\mu_c}\dfrac{\rho_w}{\rho_b}\left(\dfrac{v_w}{v_b}\right)^2\dfrac{G(\phi)^{1.8}}{F(\phi)}\right]^{1/2} + \phi + \dfrac{G(\phi)}{F(\phi)}} \right\}^{1/2}$ χ by [22] $\Phi_a = \chi^2\dfrac{\mu_w}{\mu_b}\dfrac{G(\phi)}{(1-\tilde{D}_c^2)^2}; \quad G(\phi) = \dfrac{\alpha_c - (1-\alpha_c)\phi}{\alpha_c + \alpha_w - 1}$ χ by [22]	$\tilde{D}_c = \left(\dfrac{\phi}{\phi\chi + \phi + 1} \right)^{1/2}$ $\Phi_a = \dfrac{K_1}{\phi}\left[\dfrac{(K_1\phi)^{1/2} + \phi + 1}{(K_1\phi)^{1/2} + 1} \right]^1,$ $K_1 = \dfrac{0.046}{16}\dfrac{\mu_b}{\mu_a}\mathrm{Re}_{bs}^{0.8};$ or $\Phi_a = \dfrac{K_2}{\phi^{1.8}}\left(\dfrac{K_2^{1/2}\phi^{0.1} + \phi + 1}{K_2^{1/2}\phi^{0.1} + 1} \right)^2,$ $K_2 = \dfrac{0.046}{16}\left(\dfrac{\mu_b}{\mu_a}\right)^{0.2}\left(\dfrac{\rho_b}{\rho_a}\right)^{0.8}\mathrm{Re}_{as}^{0.8}$

the optimal input volumetric ratio ϕ_m, which yields the maximum pressure reduction, are obtained as long as the core phase is laminar. Thus, for L–L flows, utilizing Φ_a (given in table 1) yields:

$$\phi_m = \left(\frac{1 + K_1^{1/2}}{1 - K_1}\right)^2; \quad \phi_m(K_1 \to 0) = 1; \quad K_1 = \frac{\mu_b}{\mu_a}; \qquad [25]$$

and for the turbulent annular phase and a laminar core with constant Re_{bs} the optimal ϕ reads

$$\phi_m = \left(\frac{1 + K_1^{1/2}}{1 - K_1}\right)^2; \quad K_1 = \frac{0.046}{16}\frac{\mu_b}{\mu_a}\mathrm{Re}_{bs}^{0.8}. \qquad [26]$$

No simple analytic expression is obtained for ϕ_m under turbulent annulus–laminar core conditions with constant Re_{as}. It is also to be noted that since the reference pressure drop, used in the definition of Φ_{as}, is that of a pure core phase, which for laminar flow is linearly dependent on the volumetric input rate, [25] and [26] also yield the conditions of the maximum flow rate of the core phase per unit two-phase pressure gradient, $Q_a/(\mathrm{d}P/\mathrm{d}x)_{\mathrm{TP}}$.

The maximum power reduction (minimum power requirement for a given oil throughput) is obtained by solving for ϕ_{mp} satisfying

$$\frac{\partial}{\partial\phi}\left[\Phi_a\left(1 + \frac{1}{\phi}\right)\right]_{\phi = \phi_{\mathrm{mp}}} = 0. \qquad [27]$$

Substituting Φ_a (given in table 1) in [27] (with $K_1 = \mu_b/\mu_a$ for a laminar annular layer or $K_1 = (0.046/16)(\mu_b/\mu_a)\mathrm{Re}_{bs}^{0.8}$ for a turbulent annular layer) yields for either L–L or T–L flows:

$$\phi_{\mathrm{mp}}^2(1 + K_1) + 3\sqrt{K_1\phi_{\mathrm{mp}}^3} - \phi_{\mathrm{mp}}(2K_1 + 1) - 4\sqrt{K_1\phi_{\mathrm{mp}}} - 2 = 0. \qquad [28]$$

For $\mu_b/\mu_a \to 0$, [28] yields $\phi_{\mathrm{mp}} = 2$.

4. RESULTS AND DISCUSSION

The calculated results presented below relate to *horizontal* annular flow of pure core and wall phases (α_c, $\alpha_w = 1$), since data or modeling of the mutual entrainment between the two phases are unavailable at the present time. In presenting the results, the relations of *in situ* hold-up and pressure drop to the nondimensional two-phase flow parameters, ϕ and χ_s^2, are discussed first. Then, comparisons with the available experimental data follow.

General effects of $\chi_s^2 - \phi$

Figures 2 and 3 present the effects of the density and viscosity ratios on the core diameter and two-phase pressure drop as functions of the χ_s^2 parameter for constant ϕ-lines. The liquid pairs chosen for demonstration in figures 2 and 3 are those of the available experimental data used below (Charles *et al.* 1961; Oliemans 1986). For a given superficial velocities ratio, $\phi = U_{as}/U_{bs}$, the extreme points, denoted by $\bigcirc$, and $\bullet$, relate to laminar flows (L–L) and turbulent flows (T–T), respectively. As the L–T transition has been found to take place earlier in two-phase flow [see, for example, Stellmach & Lilleleht (1972)], the transitional Reynolds number has been taken here as 1500.

Starting with sufficiently low flow rates, where laminar regimes prevail in both layers, $\chi^2 = \chi_s^2$ and is determined by ϕ, as indicated by [19]. Increasing the flow rates, while maintaining ϕ constant, the L–L points (nondimensional pressure drop and hold-up) remain unchanged as long as the laminar regimes prevail in both phases. Thus, point L–L represents a range of laminar flow rates. With a further increase in the flow rates, a point is reached where one of the layers becomes turbulent, and thus the ϕ-line represents L–T or T–L flows, along which ϕ and χ_s^2 are independent parameters (as indicated by [21] and [22]). As the second layer too becomes turbulent, point T–T is reached, beyond which χ_s^2 and ϕ are again dependent parameters as seen by [20], corresponding to the high flow rates range. Clearly, for a given ϕ-line, there exists a range of χ_s^2(L–L) $\leqslant \chi_s^2 \leqslant \chi_s^2$(T–T) defined by [19] and [20], where [11] yields physical solutions, between the points shown as $\bigcirc$ and $\bullet$. The intersection of [19] and [20] yields

$$\phi = \phi_{IP} = \frac{v_a}{v_b}; \quad [\chi_s^2]_{IP} = \frac{\dfrac{1}{\phi_{IP}}}{\dfrac{\mu_a}{\mu_b}} = \frac{\dfrac{\rho_a}{\rho_b}}{\left(\dfrac{\mu_a}{\mu_b}\right)^2}. \tag{29}$$

For $\phi < \phi_{IP}$, χ_s^2 is increasing with the increasing flow rates towards the turbulent regimes. On the other hand, for $\phi > \phi_{IP}$, increasing the flow rates is associated with decreasing χ_s^2. Therefore, the
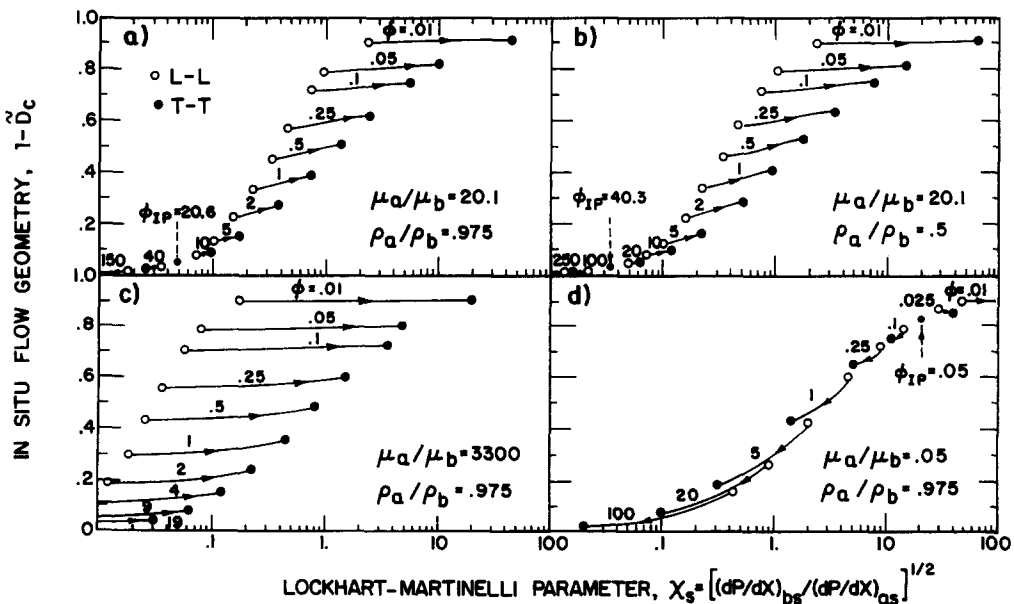
Figure 2. Core flow geometry—effect of fluid flow rates and physical properties.
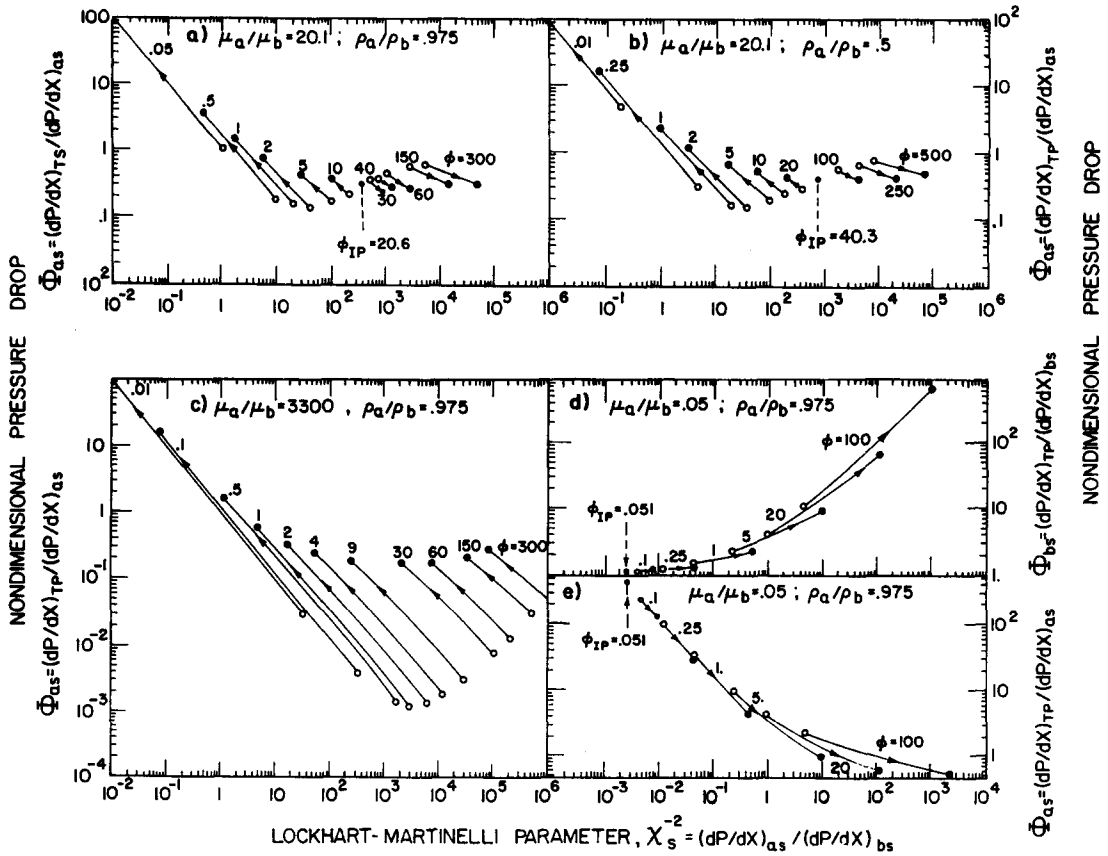
Figure 3. Nondimensional pressure drop—effect of fluid flow rates and physical properties.

intersection point (defined by $\phi = v_a/v_b$) is denoted here as the inversion point, IP. This point is easily identified in figures 2 and 3, where the arrows denote the direction of increasing flow rates at a given ϕ, moving from L–L to L–T or T–L regimes, and finally to T–T regimes. Note that with $\phi = \phi_{IP}$, as the two-fluid flow rates are increased, moving from laminar to turbulent regimes, the solutions for $\tilde{D}_c$ and the corresponding values of Φ_a and Φ_b change along a vertical line, since χ_s remains unchanged, while the solutions of [11] are functions of the flow regimes too (through n_c and n_w).

A more detailed discussion concerning the hold-up and two-phase pressure drop at and around the inversion point is given by Brauner & Moalem Maron (1989). Here, however, it is to be noted that the choice of the more viscous phase as a reference for the two-phase pressure drop (figure 3) is for the purpose of presenting the two-phase pressure drop in terms of pressure reduction, as often referred to in liquid–liquid studies. As seen in figure 3(a–c) a pressure reduction is possible for $\mu_a/\mu_b > 1$, whereas figure 3(d) demonstrates that no pressure reduction is obtained when the more viscous fluid flows in the annular gap, $\mu_a/\mu_b < 1$. Obviously, for $\mu_a/\mu_b < 1$ as $\phi \to 0$ (no addition of less viscous phase a), $\Phi_{bs} \to 1$. Also, the trend in figure 3(d), with the more viscous phase in the annular gap, is different. The trend is maintained when the pressure drop is normalized with respect to the core phase, as in figure 3(e). But since in this case Φ_{as} refers to the superficial pressure drop of the less viscous phase, it is not termed as pressure reduction. Note that, though core annular flow with a less viscous core yields no pressure reduction, it is also feasible and of practical interest as a way of protecting the conduit walls from corrosion or scale deposition effects (Hasson & Nir 1969; Hasson et al. 1970). Actually, gas–liquid annular flows represent one extreme of a less viscous core phase of $\mu_a/\mu_b \ll 1$.

Inspection of figures 2 and 3 raises some points of interest. For $\mu_a/\mu_b \gg 1$ the in situ hold-up at a given ϕ is insensitive to the χ_s parameter, which implies that the core diameter remains practically unchanged with the flow rates or the flow regimes as long as the input volumetric ratio is constant. On the other hand, the two-phase pressure drop is determined by both ϕ and χ_s [see figures 2 and

3(a–c)]. Therefore, the Lockhart–Martinelli parameter, χ_s^2, cannot be used as the single correlative parameter in liquid–liquid systems, where usually $\mu_a/\mu_b > 1$. As the viscosity ratio decreases, $\mu_a/\mu_b < 1$, as in figures 2(d) and 3(d), the general trends of the hold-up and pressure drop are different, and resemble those obtained in stratified flows, where the effect of ϕ for a given χ_s is relatively small (Brauner & Moalem Maron 1989). Thus, experimental data can be reasonably correlated only by the χ_s^2 parameter, as originally suggested for gas–liquid systems.

It is, however, to be noted that the results calculated above cover parametrically wide ranges of ϕ and χ_s which may be beyond the transitions to other flow patterns. This is dealt with elsewhere (Brauner & Moalem Maron 1991b).

Comparison with experimental data

Having demonstrated the general characteristics of the calculated results, a comparison with two available sets of data for annular liquid–liquid systems at relatively low viscosity ratios (Charles *et al.* 1961) and high viscosity ratios Oliemans (1986) is presented in figures 4–7. Since the Charles *et al.* data relate to various flow patterns, only points which are in the range of annular flow have been chosen for comparison. As seen in figures 4 and 5, the agreement of the calculated hold-up range (L–L to T–T flows) with the measured values is fairly satisfactory for the wide range of viscosity ratios. As the viscosity ratio increases, both the data and the predicted results approach the line $1 - \tilde{D}_c^2 = R = 1/(1 + \phi)$ (see [23]). Note that, since the data in figure 5 correspond mainly to turbulent water–laminar oil (where ϕ and χ_s are independent parameters), the scattering of the experimental data is to be attributed to the various (unreported) water Reynolds numbers and to the viscosity range ($\mu_a/\mu_b = 1500$ to 8000). However, as the present prediction model indicates, for a high viscosity ratio, $\mu_a/\mu_b > 1500$, the effect of the viscosity ratio on the *in situ* hold-up at L–L as well as T–T conditions becomes moderate.

Figure 6 represents the predicted two-phase pressure drop corresponding to the 5 cm tube experimental set reported by Oliemans (1986). As the data include various input volumetric oil/water ratios, $R = 0.05$ to 0.20 ($\phi \approx 19$ to 4), the calculated results are represented by a shaded area, which is in reasonable agreement with the measured pressure drop data. The experiments, as well as the predictions, yield an increasing two-phase pressure drop upon reducing the input water/oil ratio, and both are above the corresponding pressure drop that would have resulted with pure water flowing at an identical mixture velocity. The consistently higher values of the experimental data are understandable in view of the simple model used here, which utilizes smooth pipe correlations for estimating the wall and interfacial friction factors. Further improvements may depend on the availability of more sophisticated relations for τ_i (and τ_w) for the specific system studied.

As is more practical in liquid–liquid systems, the two-phase pressure drop is usually discussed in terms of pressure drop reduction compared with the superficial pressure drop of the more viscous phase, Φ_{as}. This is shown in figure 7 for the various input water fractions and specified superficial oil velocities in the 5 and 20 cm tube diameters used in Oliemans' (1986) experimental set-up. For
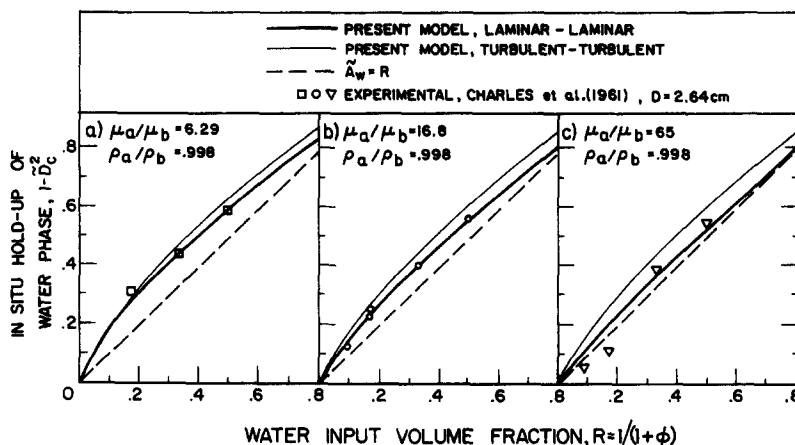
Figure 4. *In situ* hold-up—comparison with the experimental data of Charles *et al.* (1961).
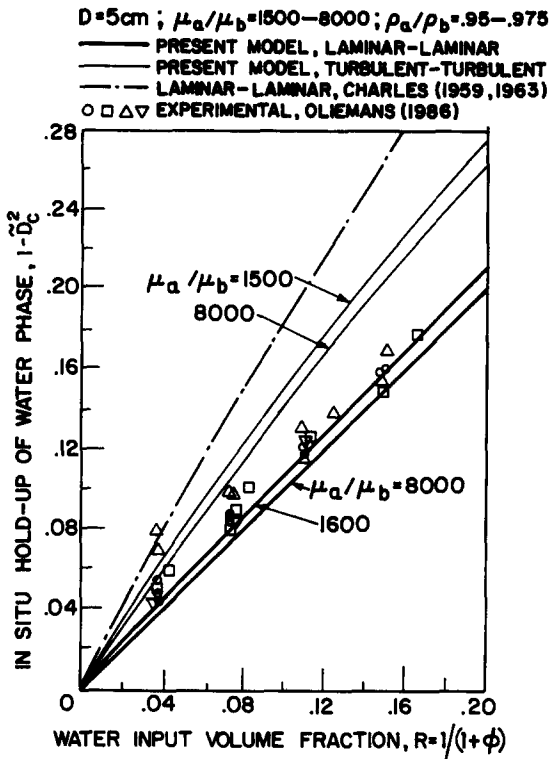
Figure 5. *In situ* hold-up—comparison with the experimental data of Oliemans (1986).
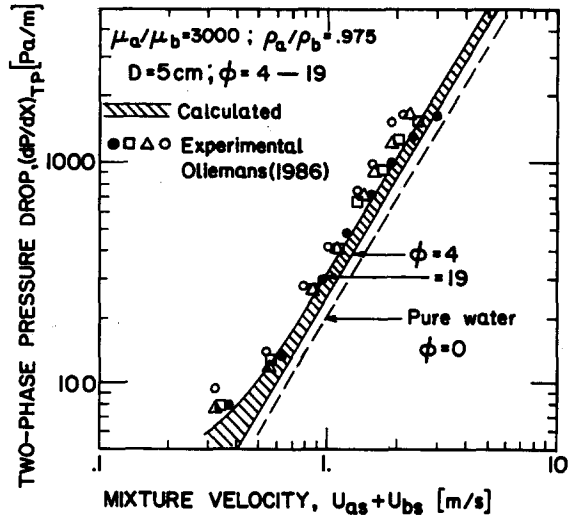
Figure 6. Two-phase pressure drop—comparison with the experimental data of Oliemans (1986): $\bigcirc$, $\phi = 19$; $\triangle$, $\phi = 9$; $\square$, $\phi = 5.67$; $\bullet$, $\phi = 4$.

the 5 cm tube, the calculated results are obtained at $U_{as} = 105$ cm/s (the experimental range is 97–110 cm/s) and for viscosity ratios of 2300 and 3300, which cover the experimental range. The predictions by the present model for the 5 cm pipe [figure 7(a)] are fairly good. For the 20 cm pipe, however, the model for the smooth pipe underestimates the measured values [figure 7(b)]. This can
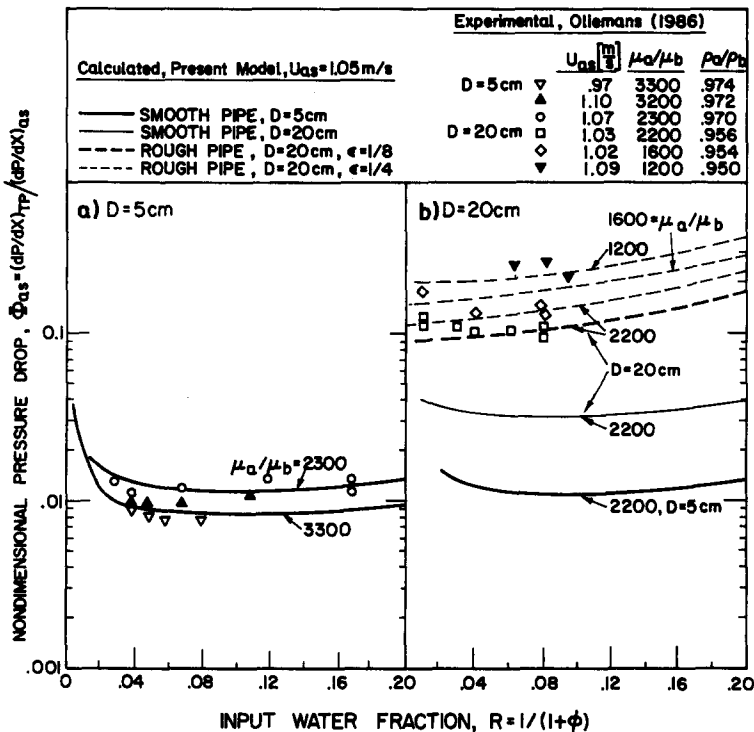
Figure 7. Pressure drop reduction—comparison with the data of Oliemans (1986) ($D = 5$ and 20 cm).

be explained by recalling the difference in roughness which might exist between the two pipes. While the 5 cm pipe represents laboratory conditions, the 20 cm pipe (reported to be 888 m long, with 22 right-angle bends) actually represents field operational conditions at a higher pipe roughness level. The increased roughness is to be attributed not only to manufacturing differences (clean pipe roughness scale), but also to the possible contamination of the pipe wall by the highly viscous wavy oil core, which is unavoidable in field operation. For the annular flow under consideration, contamination may take place as the wave amplitude is of the order of the water annular gap, and so is the resulting roughness scale, $dr \simeq h_w/2 \div h_w$, with $h_w = (D - D_c)/2$. Figure 7(b) includes calculated results for smooth, as well as rough large pipes, with $\epsilon = dr/D_w \approx 1/8$ to $1/4$, which yields fully rough surface conditions with $f_w = 2/(3.2 - 2.46 \ln \epsilon)^2$ (Davies 1972). Thus, the inclusion of the enhanced roughness effect (compared with smooth laboratory conditions), yields a reasonable prediction for the large pipe experimental set as well. It is to be noted that for highly viscous core flow, the two-phase pressure drop is mildly dependent on the specific modeling of the interfacial friction factor, since the *in situ* velocities of both phases are predicted to approach the mixture velocity and $(U_c - U_w) \to 0$ in [7]. Therefore, a possible increase in the interfacial friction factor due to interfacial waves is unlikely to be the reason for the high pressure drop observed in the field data.

In general, following figure 7(a,b), the pressure reduction (which shows a flat minimum) is practically insensitive to the less viscous fluid input ratio, provided a critical fraction (about 2–4% water) is exceeded. Both the prediction and observations indicate that a remarkable pressure reduction can be obtained in a core flow pattern, and the pressure loss saving increases as the viscosity ratio increases.

Scale-up and core flow performance

The effects of the superficial oil velocity and pipe diameter are further demonstrated in figure 8. Both effects are combined by comparing annular oil–water flows of identical oil superficial Reynolds number and identical input water/oil fraction. As expected by the nondimensional analysis in section 2, the pressure drop ratio, Φ_{as} is uniquely dependent on ϕ at the L–L regime (and diameter independent), while in the L–T regime it depends on both ϕ and Re_{as} (or ϕ and Re_{bs}). Reducing the superficial oil velocity or the pipe diameter (reducing Re_{as}) extends the range of the L–L flow regime to higher rates of water addition. In this range of water input ratios, the pressure reduction monotonously decreases towards its minimum (see figure 8). However, for higher superficial oil velocity or larger pipe diameter, the departure to the laminar oil–turbulent water flow regimes occurs at a lower input water fraction, beyond which the pressure reduction trend is flat,
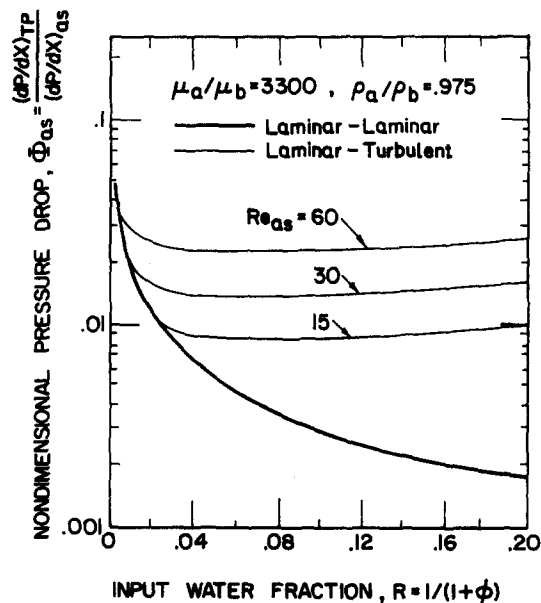
Figure 8. Pressure drop reduction for constant oil Reynolds number.

with lower pressure loss savings. Clearly, for identical oil rates and pipe diameter, the inclusion of wall roughness (in the turbulent water regime) reduces even further the potential of pressure loss savings.

The parameter which is of greatest practical interest is undoubtedly the pipe diameter, the effect of which refers to the problem of scale-up. Figure 9 represents the maximum pressure drop reduction (obtained at the minimum of figure 8) and the corresponding input water fraction, as a function of the tube diameter for constant superficial oil velocity. The required fraction of the less viscous liquid for obtaining the maximum pressure reduction varies only mildly with the tube diameter for pipes with $D > 5$ cm and, on average, is about ~ 8–9%. This is in excellent agreement with the observed range of 8–10% (Oliemans 1986). Note that for a given U_{as}, the minimum point is obtained with laminar oil–turbulent water conditions (figure 8). For rough pipes the minimum corresponds to the L–T transition point.

The two-phase pressure drop ratio (at the maximum pressure reduction), figure 9(a), demonstrates a monotonous increase with the pipe diameter, for any given oil superficial velocity, hence the pressure drop reduction decreases. Also, increasing the oil superficial velocity (at a given diameter) adversely affects the potential of pressure drop reduction.

The scale-up problem in evaluating the potential of a core flow configuration for achieving pressure reduction is more clearly demonstrated by exploring the pressure factor Π, defined in [16]. Its variation with the tube diameter and the fluid viscosity ratio is demonstrated in figure 10 for a constant oil flow rate ($U_{as} = 100$ cm/s) and about 1 and 10% water ($\phi = 10$ and 100). As long
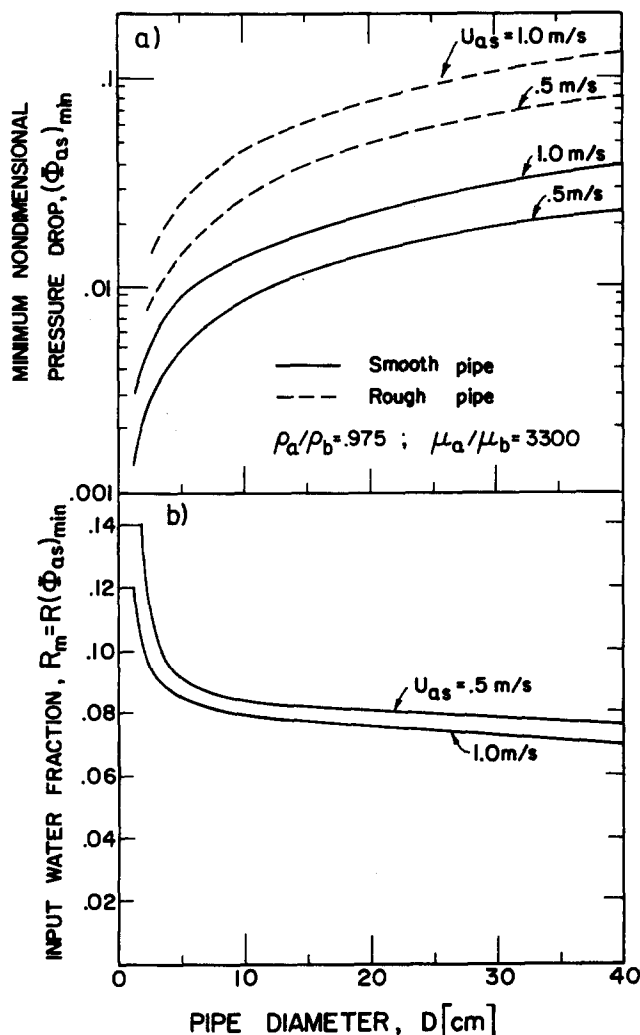
Figure 9. Maximum pressure drop reduction for constant oil flow—effect of tube diameter.
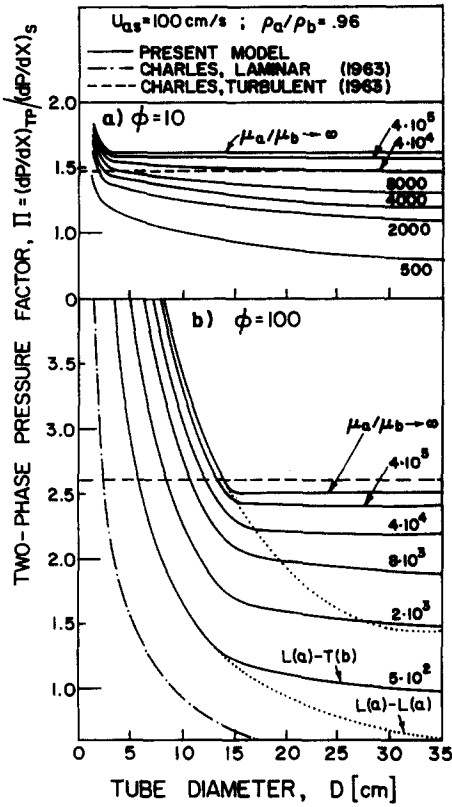
Figure 10. The effect of tube diameter and oil viscosity on the two-phase pressure factor.
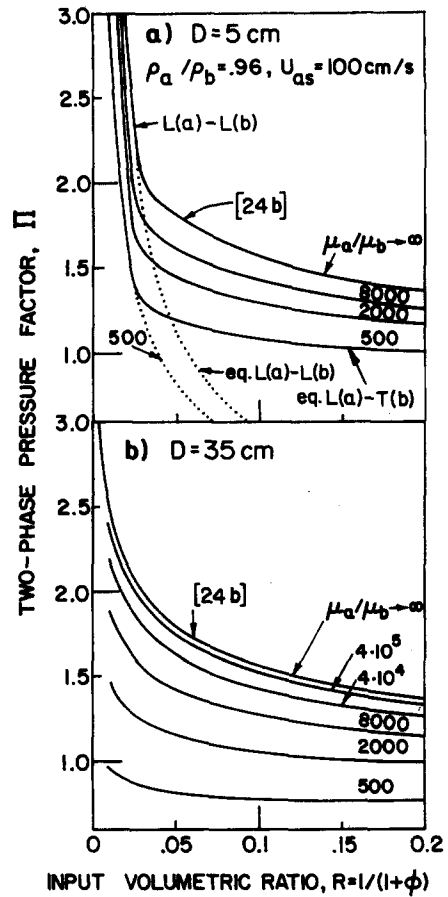
Figure 11. The effect of input volumetric ratio and oil viscosity on the two-phase pressure factor.

as laminar flow is maintained in the annular gap (small D) the pressure factor decreases with increasing tube diameter. When turbulence develops in the water annulus (higher D), the pressure factor levels off and its value becomes almost independent of the tube diameter. The evaluation (solid curves) is based on a transitional Reynolds number $Re_w = D_w u_w / v_w = 1500$. The dotted curves mark the Π values that would have been obtained with an annular laminar layer maintained at higher Reynolds numbers.

Figure 10 shows that for a sufficiently low viscosity ratio, a value of $\Pi < 1$ may be reached, indicating that the two-phase pressure drop may be even less than the pressure drop evaluated for water flowing alone at the mixture velocity. With increasing oil viscosity, the pressure factor increases, approaching the asymptotic values predicted for $\mu_a/\mu_b \to \infty$ by [24a,b]. Hence, for extremely waxy oils, the pressure factor Π is independent of the tube diameter as long as a turbulent annular layer is assured.

The effect of the percentage of water added is further demonstrated in figure 11. It is shown that while for a laminar water annulus the pressure ratio sharply decreases with increasing the water addition, its sensitivity to ϕ is much less pronounced with turbulent flow in the annular layer.

Comparison with capsule models

It is of interest to refer at this point to various capsule models available in the literature (Charles 1963; Newton et al. 1964). These models treat either laminar or turbulent flow in the annular gap, formed by the free flow of a solid core in tubes. The present model, which accounts for the core viscosity, converges, in fact, to a capsule flow model in the limit of highly waxy core flow, with $\mu_a/\mu_b \to \infty$. Figures 10–12 show a comparison between the pressure factor predicted by the present model with Charles' (1963) laminar and turbulent capsules models. The lower values of Π obtained
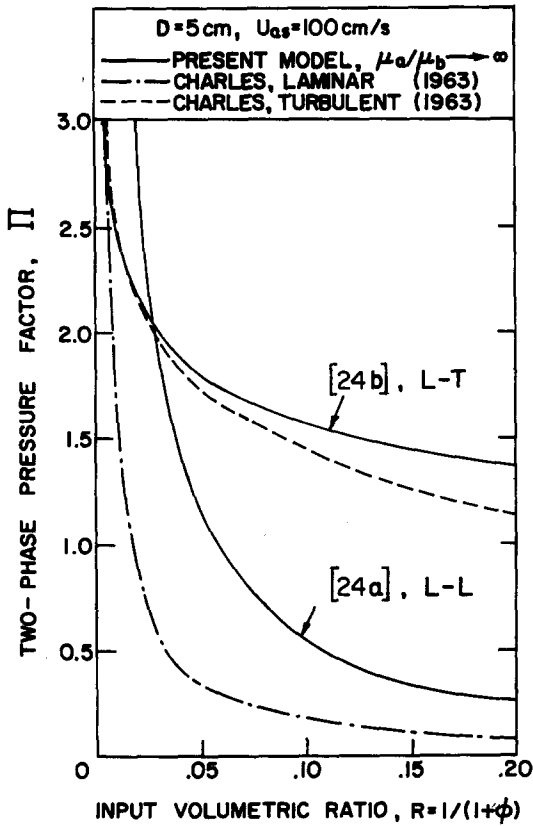
Figure 12. The two-phase pressure factor for $\mu_a/\mu_b \to \infty$: comparison with the capsule models of Charles (1963).
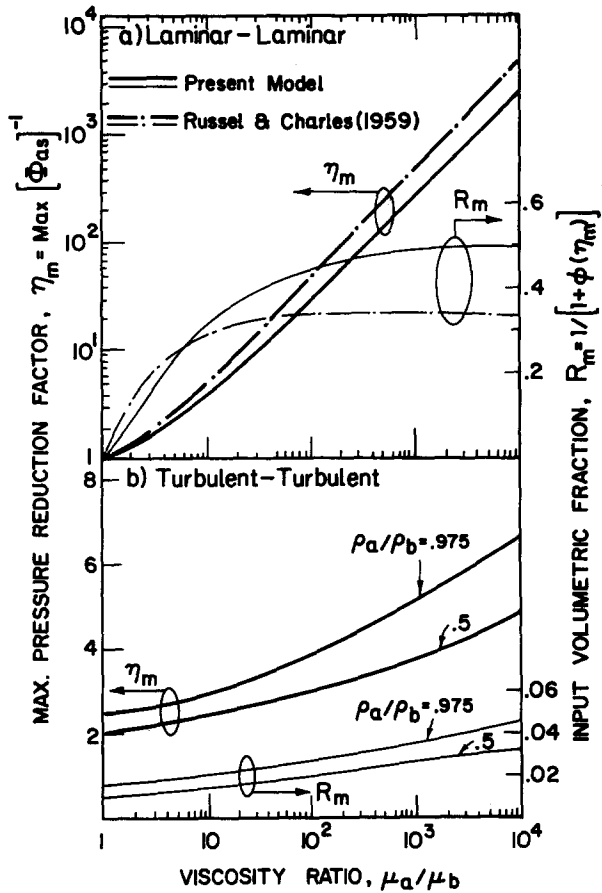
Figure 13. Maximum pressure drop reduction factor and the corresponding input volumetric ratio for L–L and T–T flows.

with Charles' (1963) laminar capsule model are an outcome of the higher predicted values of the *in situ* water hold-up, as shown in figure 5.

For a turbulent annular phase, closer agreement between Charles (1963) and the present model is noticed. It is to be noted that Charles' turbulent capsule model, which is based on the 7th power-law velocity distribution in the annular gap, also yields a diameter-independent pressure factor (see figure 10). Moreover, both models show a monotonous decrease of Π with increasing water addition. With laminar flow in the annular gap a pressure factor < 1 may be reached, even with extremely waxy oil cores. Yet, with a turbulent annular phase, the value of the pressure factor is always of the order of 1, indicating that capsules and very viscous oils may be transported with pressure losses almost identical to those of water flow at the combined two-phase volumetric rate, provided a core flow configuration can be maintained.

Optimal pressure drop and power reduction

As a summary, the maximum pressure drop reduction factor, $\eta_m \simeq \max(\Phi_{as})^{-1}$ and the corresponding volumetric input ratio of the less viscous phase added, $R_m = 1/(1 + \phi_m)$, are presented in figure 13 for the L–L and T–T extremes and various fluids pairs. Included, for comparison, is the Russell & Charles (1959) L–L solution. Also, presented in figure 14 is the maximum possible power reduction which is related to the pressure drop reduction by $\psi_m = \max(\Phi_{as}^{-1}(\phi/1 + \phi))$.

Clearly, the potential of pressure drop or power savings with the addition of a less viscous phase increases as the transported core becomes more viscous. Under the conditions of laminar flow in both phases, the solution is independent of the fluid densities. For turbulent conditions, as the density difference between the core and annular phases decreases, the possible reduction increases. It is to be noted also that the pressure and power reduction under laminar conditions are much
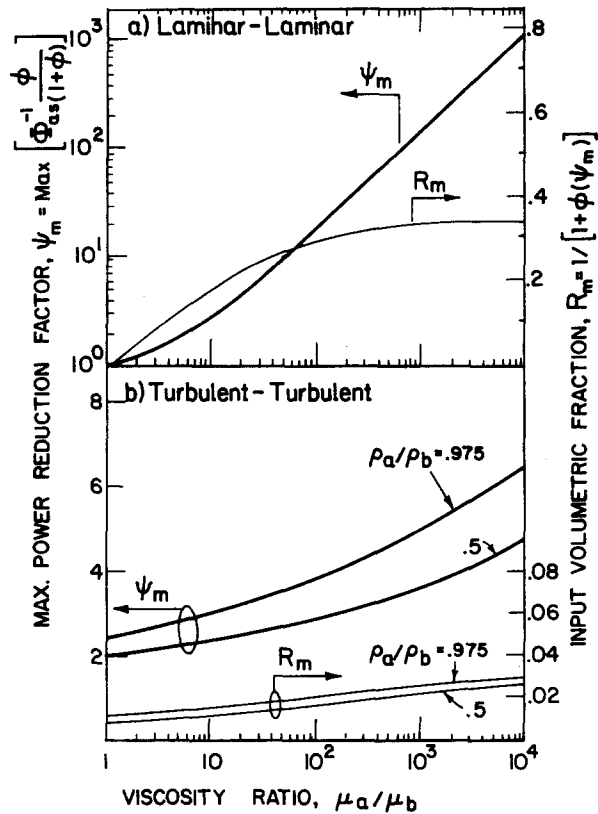
Figure 14. Maximum power reduction factor and the corresponding input volumetric ratio for L–L and T–T flows.

higher than those expected in turbulent flows. For mixed flow regimes, the reduction potential is between the L–L and T–T extremes. Clearly, for a highly viscous core, the core phase is practically always laminar. Consequently, only L–L or turbulent annulus–laminar core flows are relevant, whereas the T–T extreme is introduced here only as a limiting bound.

5. CONCLUSION

A model for predicting the pressure drop and *in situ* hold-up associated with the annular flow of two immiscible liquids in a horizontal pipe is presented. This flow pattern appears to be the most attractive as a way of reducing pressure losses and power requirements in the transportation of highly viscous oils with water injected into the pipe forming a lubricating annular layer.

Nondimensional analysis shows that, in contrast to gas–liquid flows, where pressure drop and hold-up are well-correlated by the Martinelli parameter χ, liquid–liquid systems are generally dependent on both χ and the fluid flow rate ratio ϕ. This dependence is demonstrated for various fluids pairs, defined by the viscosity and density ratios $(\mu_a/\mu_b, \rho_a/\rho_b)$, and for a wide range of flow rates covering all possible flow situations of L–L, T–T or mixed flow regimes.

Simple explicit expressions are derived for the pressure drop and hold-up associated with a laminar core (with either a laminar or turbulent annular layer). In the limit of a highly viscous core, $\mu_a/\mu_b \to \infty$, the present model converges to a solid capsule flow model, in which case the *in situ* velocities of both phases approach the mixture velocity, while the hold-up equals the input volumetric ratio. The corresponding pressure drop is comparable to that which would have been obtained with the less viscous fluid (water) flowing alone in the pipe at the combined mixture velocity. The pressure drop ratio is found to be independent of the tube diameter as long as a turbulent annular layer is maintained.

In field operations, core flow configurations may demonstrate a lesser pressure reduction, due to possible contamination of the tube wall by the waxy oil. It is shown, however, that the present

model can be successfully extended to field conditions by introducing a fully rough surface model for the wall shear friction factor.

Finally, it is to be noted that although the results presented cover wide ranges of operational liquid–liquid flow conditions, it is not assured that the annular configuration can always be maintained. The region of stable annular liquid–liquid flow and the transition boundaries to other possible flow patterns are the subject of subsequent papers (Brauner 1990; Brauner & Moalem Maron 1990, 1991a–c).

REFERENCES

BENTWICH, M. 1964 Two-phase viscous axial flow in a pipe. *J. bas. Engng Trans. ASME Ser. D* **86**, 669–672.

BENTWICH, M., KELLY, D. A. I. & EPSTEIN, N. 1970 Two-phase eccentric interface laminar pipeline flow. *J. bas. Engng Trans. ASME Ser. D* **92**, 32–36.

BRAUNER, N. 1990 On the relations between two-phase flow under reduced gravity and earth experiments. *Int. Commun. Heat Mass Transfer* **17**, 271–282.

BRAUNER, N. & MOALEM MARON, D. 1989 Two-phase liquid–liquid stratified flow. *PhysicoChem. Hydrodynam.* **11**, 487–506.

BRAUNER, N. & MOALEM MARON, D. 1990 Stability, well-posedness and flow pattern transitions in two-phase liquid–liquid flows. Presented at the *6th Miami Int. Symp. on Heat and Mass Transfer*, Miami, Fla.

BRAUNER, N. & MOALEM MARON, D. 1991a Stability of two-phase liquid–liquid stratified flow. *Int. J. Multiphase Flow*. Submitted.

BRAUNER, N. & MOALEM MARON, D. 1991b Two-phase liquid–liquid flow pattern transition in horizontal flows. *Int. J. Multiphase Flow*. Submitted.

BRAUNER, N. & MOALEM MARON, D. 1991c Analysis of stratified/nonstratified transitional boundaries in horizontal gas–liquid flows. *Chem. Engng Sci*. In press.

CHARLES, M. E. 1963 The pipeline flow of capsules—part 2: theoretical analysis of the concentric flow of cylindrical forms. *Can. J. chem. Engng* **41**, 46–51.

CHARLES, M. E., GOVIER, G. W. & HODGSON, G. W. 1961 The horizontal pipeline flow of equal density oil–water mixtures. *Can. J. chem. Engng* **39**, 27–36.

DAVIES, J. T. 1972 *Turbulence Phenomena*. Academic Press, New York.

ELLIS, H. S. 1964a The pipeline flow of capsules—part 3. An experimental investigation of the transport by water of single cylindrical and spherical capsules with density equal to that of the water. *Can. J. chem. Engng* **42**, 1–8.

ELLIS, H. S. 1964b The pipeline flow of capsules—part 4. An experimental investigation of the transport in water of single cylindrical capsules with density greater than that of the water. *Can. J. chem. Engng* **42**, 69–76.

ELLIS, H. S. 1964c The pipeline flow of capsules—part 5. An experimental investigation of the transport by water of single spherical capsules with density greater than that of the water. *Can. J. chem. Engng* **42**, 155–161.

ELLIS, H. S. & BOLT, L. H. 1964 The pipeline flow of capsules—part 7. An experimental investigation of the transport by two oils of single cylindrical and spherical capsules with density equal to that of the oil. *Can. J. chem. Engng* **42**, 201–206.

HASSON, D. & NIR, A. 1969 Annular flow of two immiscible liquids—analysis of core–liquid ascent. Presented at the *A.I.Ch.E 66th natn. Mtg*, Portland, Ore.

HASSON, D., MANN, U. & NIR, A. 1970 Annular flow of two immiscible liquids; I. Mechanisms. *Can. J. chem. Engng* **48**, 514–520.

KRUYER, J., REDBERGER, P. J. & ELLIS, H. S. 1967 The pipeline flow of capsules—part 9. *J. Fluid Mech.* **30**, 513–531.

MOALEM MARON, D., BRAUNER, N. & KRUKA, V. R. 1990 A new mechanism for highly viscous core flow. Presented at the *6th Miami Int. Symp. on Heat and Mass Transfer*, Miami, Fla.

NEWTON, R., REDBERGER, P. J. & ROUND, G. F. 1964 The pipeline flow of capsules—part 6. Numerical analysis of some variables determing free flow. *Can. J. chem. Engng* **42**, 168–173.

OLIEMANS, R. V. A. 1986 The lubricating-film model for core–annular flow. Ph.D. dissertation, Delft Univ.

OOMS, G. 1972 The hydrodynamic stability of core–annular flow of two ideal liquids. *Appl. scient. Res.* **26,** 147–158.

OOMS, G. & BECKERS, H. L. 1972 The flow of a rigid core surrounded by an annular liquid layer through a horizontal tube. *Appl. scient. Res.* **26,** 321–334.

OOMS, G., SEGAL, A., VAN DER WEES, A. J., MEERHOFF, R. & OLIEMANS, R. V. A. 1984 A theoretical model for core–annular flow of a very viscous oil core and a water annulus through a horizontal pipe. *Int. J. Multiphase Flow* **10,** 41–60.

OOMS, G., SEGAL, A. & CHEUNG, S. Y. 1985 Propagation of long waves of finite amplitude at the interface of two viscous fluids. *Int. J. Multiphase Flow* **11,** 481–502.

REDBERGER, P. J. & CHARLES, M. E. 1962 Axial laminar flow in a circular pipe containing a fixed eccentric core. *Can. J. chem. Engng* **40,** 148–151.

ROUND, G. F. & BOLT, L. H. 1965 The pipeline flow of capsules—part 8. An experimental investigation of the transport in oil of single, denser-than-oil, spherical and cylindrical capsules. *Can. J. chem. Engng* **43,** 197–205.

RUSSELL, T. W. F. & CHARLES, M. E. 1959 The effect of the less viscous liquid in the laminar flow of two immiscible liquids. *Can. J. Chem. Engng* **37,** 18–24.

STELLMACH, H. S. & LILLELHT, L. U. 1972 Laminar–turbulent transition for certain stratified two-phase flows. *Ind. Engng Chem. Fundam.* **11,** 418–420.